© 2022. Published by The Company of Biologists Ltd | Development (2022) 149, dev200982. doi:10.1242/dev.200982

TECHNIQUES AND RESOURCES

RESEARCH REPORT

# Single-cell RNA-sequencing analysis of early sea star development

**Stephany Foster, Nathalie Oulhen, Tara Fresques, Hossam Zaki and Gary Wessel***

## ABSTRACT

Echinoderms represent a broad phylum with many tractable features to test evolutionary changes and constraints. Here, we present a single-cell RNA-sequencing analysis of early development in the sea star *Patiria miniata*, to complement the recent analysis of two sea urchin species. We identified 20 cell states across six developmental stages from 8 hpf to mid-gastrula stage, using the analysis of 25,703 cells. The clusters were assigned cell states based on known marker gene expression and by *in situ* RNA hybridization. We found that early (morula, 8-14 hpf) and late (blastula-to-mid-gastrula) cell states are transcriptionally distinct. Cells surrounding the blastopore undergo rapid cell state changes that include endomesoderm diversification. Of particular import to understanding germ cell specification is that we never see Nodal pathway members within Nanos/Vasa-positive cells in the region known to give rise to the primordial germ cells (PGCs). The results from this work contrast the results of PGC specification in the sea urchin, and the dataset presented here enables deeper comparative studies in tractable developmental models for testing a variety of developmental mechanisms.

**KEY WORDS: Inductive germline, Primordial germ cell (PGC), Vasa, Nanos, Sea star, Sea urchin, Cell fates, scRNA-seq**

## INTRODUCTION

Revealing the genetic regulation of cell type identity leads to a deeper understanding of the mechanisms of embryogenesis and evolutionary diversity. Studies of developmental mechanisms between closely related vertebrate and invertebrate models have been fruitful in revealing evolutionary changes that include gene duplications followed by divergence, and changes in promoter elements that shift important kernels in gene regulatory networks (Briggs et al., 2018; Davidson, 2006). The sea star and sea urchin have recently been subject to comparative analyses of developmental heterochronies, gene regulatory networks and neurogenesis (Cary et al., 2020; Gildor et al., 2017; Hinman and Burke, 2018). Sea stars and sea urchins spawn millions of gametes, which, when fertilized, will develop external to the adults. The transparent embryos can be easily cultured, treated, dissociated and analyzed in great quantities. Single-cell atlases of development to larvae in echinoderm species have been reported for the sea urchin *Strongylocentrotus purpuratus* and *Lytechinus variegatus* (Foster et al., 2020; Massri et al., 2021; Paganos et al., 2021). Here, we set out to compile a single-cell dataset from a sister taxa of the sea urchins, the sea star *Patiria miniata*, as a resource for deeper analysis of development in this animal as well as a point of comparison for other echinoderms. Of particular interest to us is the difference in germ line specification methods used between the sea urchin and sea star. Known marker genes for this and other lineages are leveraged here to reveal gene activities that become targets for new functional analysis.

Department of Molecular Biology, Cellular Biology & Biochemistry Division of BioMedicine, Brown University, Providence, RI 02912, USA.

*Author for correspondence (rhet@brown.edu)

G.W., 0000-0002-1210-9279

**Handling Editor: Cassandra Extavour**
**Received 26 May 2022; Accepted 17 October 2022**

## RESULTS AND DISCUSSION

### Identification of cell states across early sea star development

Sea star embryos were cultured to six key developmental stages; 8 h post-fertilization (hpf), 10 hpf, 14 hpf, blastula (B), early gastrula and mid-gastrula (MG) stage, at which point they were dissociated, processed for single-cell RNA-sequencing (scRNA-seq) via Drop-seq, and aligned to the *P. miniata* genome (Macosko et al., 2015). All six datasets were analyzed using Seurat and integrated using Harmony, an scRNA-seq data integration tool, to identify conserved cell types across all datasets (Korsunsky et al., 2019; Stuart et al., 2019). After quality control measures, cells from all datasets were included in the integration as follows: 8 hpf (868 cells), 10 hpf (1318 cells), 14 hpf (2448 cells), blastula (7272 cells), early gastrula (3349 cells) and mid-gastrula (10,448 cells). This analysis of 25,703 total cells yielded 20 clusters (cell states) across all time points identified by known marker gene expression and by *in situ* RNA hybridization (Fig. 1A,B; Table S6). In analyzing the six datasets together, it is evident that early (8-14 hpf) and late (B-MG) cell states are transcriptionally distinct. Cell clusters of early stages (clusters 3 and 7) decrease with development; these cells are presumably 'lost' to differentiation (Fig. S1). Clusters 3, 7 and 9, which make up the majority of the earlier stage datasets, showed enrichment of CyclinA and lack of distinct marker gene expression (Fig. 1B). This suggests that these early stage cell states harbor similar mRNA expression.

### Blastula

We assessed the blastula and gastrula stage datasets individually in greater detail using expression of key regulatory genes characterized previously. We found the time and pattern of expression was consistent with previously reported *in situ* hybridizations. In blastulae, we detected ten cell states (blastula clusters B0-B9) which were identified by expression of such known marker genes (Fig. 2A,B; Tables S1 and S3). We identified ectodermal cells by expression of *soxB1* (also known as *sox2*) (Yankura et al., 2013). *foxq2* (*foxe3l*) and *dkk3* are expressed in the animal pole domain, in which the apical organ of the nervous system will form (Cheatle Jarvela et al., 2016). Cluster B0 expresses high levels of *soxB1*, *foxq2* and *dkk3*. Cluster B1 expresses *foxq2* and *dkk3*, which we identify as the animal pole domain (Fig. S2). Although these apical

Development (2022) 149, dev200982. doi:10.1242/dev.200982

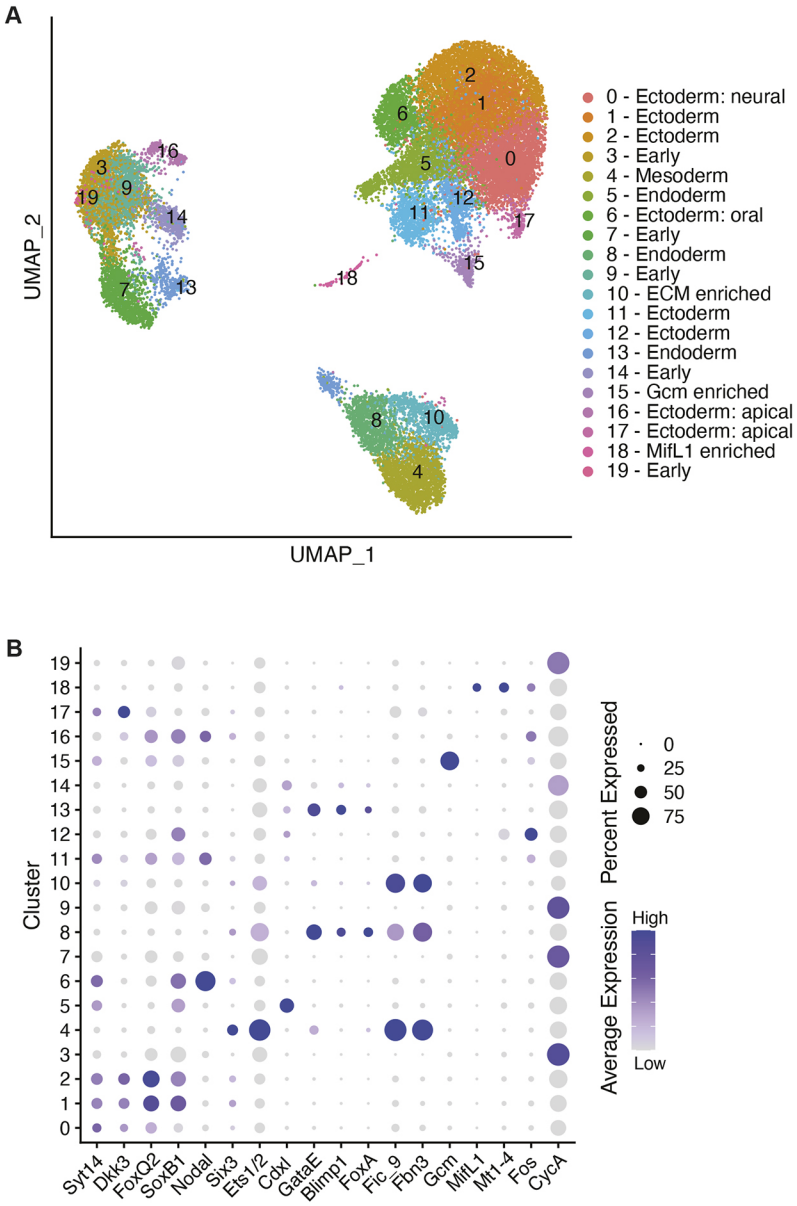


**Fig. 1. Cell states identified across early sea star development.** (A) UMAP visualization of 25,703 cells after integration of six datasets. Cells colored by cell state identity based on marker gene expression (Table S6). (B) Dot plot showing marker gene expression across clusters. Average gene expression level displayed by color intensity. Percentage of cells expressing the marker gene conveyed by circle size.

ectodermal markers are widespread in the dataset, the vegetal markers are restricted to a subset of cell states. These vegetal markers include both mesodermal and endodermal progenitors. *ets1/2* (*ets1*), a marker of the presumptive mesoderm, is expressed in the vegetal plate (Cary et al., 2020). *gataE* (*Gata6*), *foxA* (*foxa1*), *brachyury* (*tbxt*) and *blimp1* (*prdm1*), all genes involved in endodermal development, mark different regions of the embryonic gut. However, in blastulae, they are all expressed in the vegetal region, surrounding the blastopore (Fresques et al., 2014; Hinman and Davidson, 2003). *Cdxl* (*cdx1l*), another endodermal marker, is also expressed as a vegetal ring in blastulae; it is later restricted to the blastopore region in mid-gastrulae (Annunziata et al., 2013). *gataE*, *foxA* and *blimp1* are expressed in the same cluster as *ets1/2* (cluster B2), whereas *brachyury* and *cdxl* are markers of cluster B3 (Fig. 2B; Fig. S2). At blastula stage, the transcription factor *glial cells missing* (*gcm*; *gcml*), which marks the pigment cells in the related purple sea urchin, shows no localized expression; *gcm*-positive cells are present throughout the ectoderm (Calestani et al., 2003; McCauley et al., 2010). In our dataset, cells with the highest *gcm* expression clustered into a unique population in cluster B8, with some *gcm*-positive cells present within the ectodermal clusters (Fig. 2B; Fig. S2).

Expression of the Wnt signaling ligands and receptors has previously been characterized in blastula and gastrula stages (McCauley et al., 2013). As signaling plays an important role in development and inductive germline specification, we sought to include the Wnt ligand expression in our analysis. Six Wnt ligands and three Wnt Frizzled receptors are encoded in the *P. miniata* transcriptome (McCauley et al., 2013). Our dataset showed co-expression of genes encoding ligands Wnt3, Wnt16 and the Wnt receptor Frizzled1 (Fzd2) in cluster B2 (Fig. S4). These three genes are known, using *in situ* hybridization, to be expressed in the vegetal pole at blastula stage (McCauley et al., 2013). *wnt8* (*wnt8a*) is also expressed in the vegetal pole, not overlapping with *frizzled1* expression. Our analysis revealed the *wnt8* expression pattern showed overlap with *wnt3* (cluster B3) and no overlap with *wnt3* (cluster B7), mirroring what has been previously reported (Fig. S4)

Development (2022) 149, dev200982. doi:10.1242/dev.200982

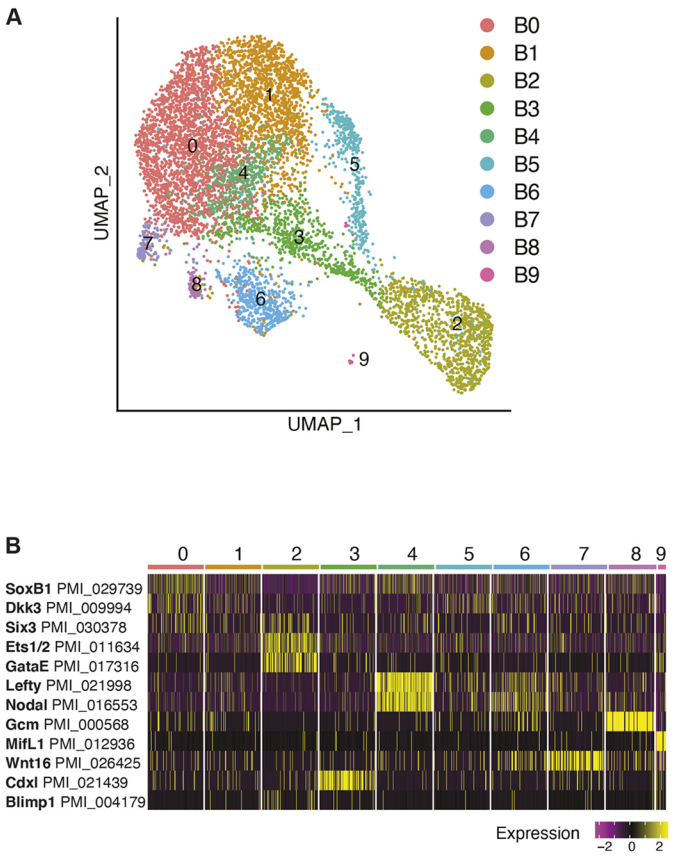


**Fig. 2. Gene expression at blastula stage.** (A) UMAP plot of 7272 blastula stage cells. Clusters colored by cell state identity based on marker gene expression (Table S3). (B) Heatmap of blastula stage marker gene expression.

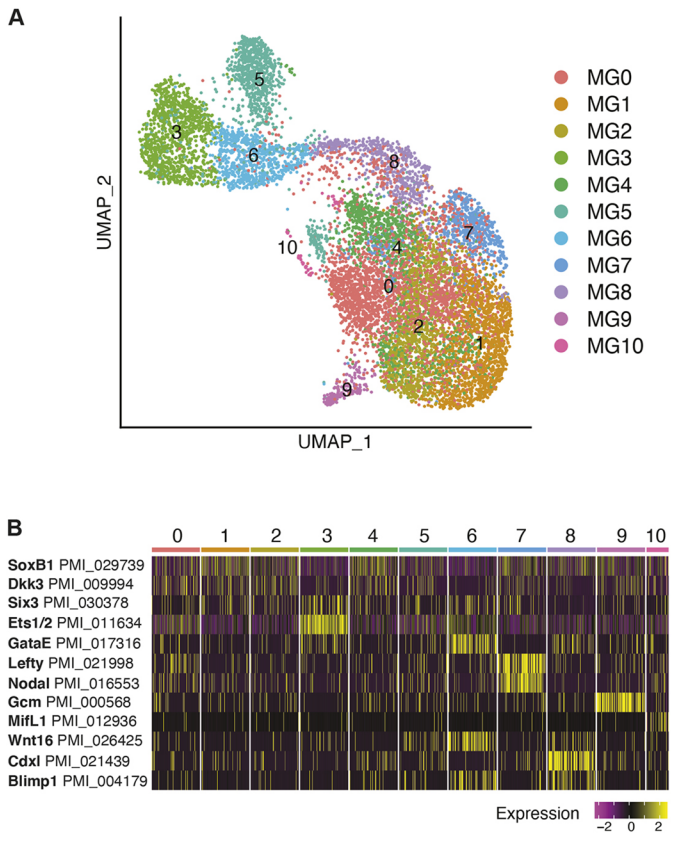


**Fig. 3. Gene expression at mid-gastrula stage.** (A) UMAP plot of 10,448 mid-gastrula stage cells. Clusters colored by cell state identified by marker gene expression (Table S4). (B) Heatmap of mid-gastrula stage marker gene expression.

(McCauley et al., 2013). We also sought to identify expression of the highly conserved germ cell markers nanos genes (*nanos2* and *nanos3*) and *vasa* (*ddx4*), the expression of which has been characterized by *in situ* hybridization (Fresques et al., 2014, 2016). *vasa* mRNA is expressed in the vegetal plate of blastulae and is particularly enriched in cluster B2, like the *wnt3* and *wnt16* ligands, and the receptor *frizzled1* (Fig. S6H) (Fresques et al., 2014). Results from both scRNA-seq and *in situ* hybridization show low or no detection of nanos in blastulae based on the threshold of these techniques (Fig. S6A) (Fresques et al., 2016).

## Mid-gastrula

Analysis of the mid-gastrula stage dataset reveals 11 cell states (mid-gastrula clusters, MG0-MG10) (Fig. 3A; Tables S1 and S4). At this stage, many characteristics of the animal ectoderm remain the same. Ectodermal cell types (clusters MG0,1,2,4) are still distinguished by expression of *soxB1*, *foxQ2* and *dkk3* (Fig. S3; Table S4). Expression of several vegetal markers detected at blastula stage now changes from overlapping to marking either vegetal ectoderm or different regions of the gut. In blastula stage, both *ets1/2* and *gataE* were expressed in the same cluster (cluster B2). At gastrula stage, *ets1/2* is particularly enriched in cluster MG3, and *gataE* marks a different cluster (cluster MG6) (Fig. 3B). *ets1/2* at gastrula stage is present at the tip of the archenteron, where it marks presumptive mesoderm and ingressing mesenchyme cells (Cary et al., 2020; Hinman and Davidson, 2007). We see low level *gataE* expression in the archenteron, although *gataE* is enriched in the mid- to hindgut region in mid-gastrula (Hinman and Davidson, 2003). *foxA*, which is expressed in the mid/hindgut region, is enriched in the same cluster as *gataE* (Hinman et al., 2003). In mid-gastrulae, *brachyury* expression surrounds the blastopore but is not within the blastopore (Hinman et al., 2003). *cdxl* expression is restricted to the region around the blastopore (Annunziata et al., 2013). *brachyury* and *cdxl* are both enriched in cluster MG8, reflecting their expression pattern seen via *in situ* hybridization (Fig. S3).

Lack of unique marker gene expression makes cluster 5 difficult to identify. Cluster MG5 showed enrichment of extracellular matrix protein expression, including fibrinogen (PMI_003448 Fic_9) and fibrillin (PMI_026729 Fbn3) (Table S4). Similar to blastula stage, one cluster is marked by high *gcm* expression, cluster MG9. A small number of cells cluster on their own (cluster MG10) and these cells are marked by macrophage inhibitory factor like 1 (*mifl1*) (Fig. 3B). MIF plays a role in immune function in vertebrates (Hibino et al., 2006; Nishihira, 2000). Cluster MG10 also expresses *mt1-4*, a metalloprotease, and *fos* (*fosl*), a transcription factor, both enriched in the sea urchin primary mesenchyme cells (PMCs) (Fig. S5A) (Rafiq et al., 2012; Sun and Ettensohn, 2014). *mt1-4* is seen at the tip of the archenteron in gastrulae by *in situ* hybridization (Fig. S5B). Further studies are necessary to reveal what role these genes play in sea star development; this is especially poignant as sea star embryos lack PMCs and pigment cells.

The sea star embryo is known to have left/right morphological asymmetry by gastrula stage. A Nodal signaling gradient on the

Development (2022) 149, dev200982. doi:10.1242/dev.200982

right side of the embryo is responsible for restricting the posterior enterocoel (PE), which houses the presumptive germ line, to the left side, as well as restricting nanos and *vasa* expression to this region (Fresques and Wessel, 2018). In our dataset, *nodal* (*nodall*) expression, along with its target *lefty* (*lefty1*), is enriched in one cluster (cluster MG7) which we identify as the right-side ectoderm (Fig. 3B) (Duboc et al., 2005). Although Nodal has been identified to inhibit germ line gene expression, the signal (or signals) that activate germ line gene expression remains unknown. In contrast to Nodal signaling, Wnt pathway component expression is present in the same region as nanos and *vasa* RNA expression in the early embryo and in the forming gut during the gastrula stage (Fresques and Wessel, 2018; Fresques et al., 2014, 2016; McCauley et al., 2013). *In situ* hybridization shows enrichment of nanos and *vasa* transcripts at the top of the archenteron and in a vegetal ring in the hindgut region at mid-gastrula stage (Fresques and Wessel, 2018; Fresques et al., 2014, 2016). Among the six Wnt ligands present in the sea star transcriptome, RNA expression patterns of *wnt3*, *wnt8* and *wntA/4* show overlap with the region of nanos and *vasa* RNA expression in the gastrula stage embryo (Fresques and Wessel, 2018; McCauley et al., 2013). Among the three Wnt receptors, *frizzled1/2/7* (*fzd2*) RNA expression is concentrated in the forming gut of the early gastrula (McCauley et al., 2013). The three signaling ligands, *wnt3*, *wnt8* and *wntA/4*, show appropriate expression patterns to be candidates for initiating germ line specification by interacting with the Frizzled1/2/7 receptor, due to their tight colocalization with the nanos and *vasa* RNA expression pattern in the early embryo. At mid-gastrula, the Wnt signaling ligands have been described as having a nested gene expression pattern. *wnt16* shows most vegetal expression followed by *wnt3* and then *wnt8* along the ectoderm. In our dataset, *wnt16* enrichment is seen in cluster MG6 with *wnt3* expression. *wnt3* is also co-expressed with Wnt8 in cluster MG8. *frizzled1* is present in cluster MG3, which we identify as the tip of the archenteron (Fig. S4) (McCauley et al., 2013).

### Derivation of the germ line cells

Origins of the germ line have a particularly important regulatory node in the mid-gastrula stage, where nanos and *vasa* are both expressed and will be restricted to the region of PE formation. The PE is posited to be the source of the germ line, as it is the source of restricted and specific germline gene enrichment in the sea star larva (Fresques et al., 2014; Fresques and Wessel, 2018). Moreover, removal of the PE via micropipetting results in larvae with significantly fewer germline cells (Inoue et al., 1992). Because of this, we sought to characterize the expression pattern of nanos and *vasa*-positive cells in mid-gastrulae. Nanos expression is detected in 267 total cells, co-expression of nanos and *vasa* is seen in 212 cells. Nanos expression is much less abundant compared with *vasa*; *vasa* expression is seen in all clusters at mid-gastrula stage, but expression in the hindgut cluster (cluster MG8) was of greatest interest to us (Fig. S6H). We took a closer look at the *vasa*-positive cells in the hindgut cluster and compared gene expression in the hindgut cells that express *vasa* with those that do not. In extracting a list of differentially expressed genes in *vasa*-positive cells of the hindgut cluster, we found the transcription factor *foxY3* (Tables S2, S5). Delta/Notch signaling in the purple sea urchin was found to regulate nanos expression through the FoxY transcription factor in somatic cells adjacent to the PGCs (Oulhen et al., 2019; Materna et al., 2013). *P. miniata* has three FoxY transcription factors and we sought to characterize their expression patterns via *in situ* hybridization. Expression of all three FoxY genes

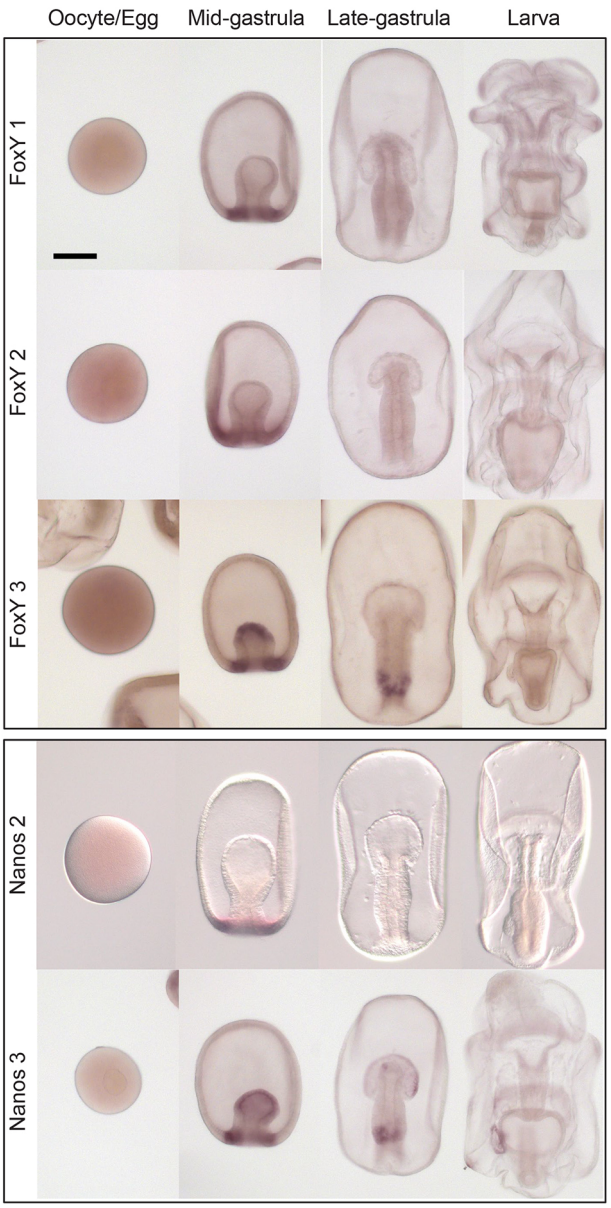


**Fig. 4. FoxY and Nanos gene expression.** Whole mount *in situ* hybridizations for Nanos and the FoxY transcription factors during early sea star embryogenesis. *nanos3* (PMI_027092; the focus of this study) expression is seen in mid-gastrula at the tip of the archenteron and the hindgut region. *nanos3* expression persists as a ring in the gut in late gastrula and becomes restricted to the PE; some expression is detected in the anterior pouches. *nanos2* (PMI_029792) is expressed transiently as a ring around the blastopore in mid-gastrula. *foxY1* (PMI_028394) and *foxY2* (PMI_008472) are also transiently expressed at mid-gastrula stage. *foxY3* (PMI_000733) is expressed in the same domain as *nanos3* at mid and late gastrula stages. At least 50 embryos from each developmental stage from three parental matings were tested. Scale bar: 100 µm.

was present at mid-gastrula, in the same region as nanos and *vasa* expression (Fig. 4; Fig. S7A). By late gastrula stage, expression of *foxY1* and *foxY2* was lost (Fig. 4). *foxY3* was expressed in the same domain as nanos and *vasa* at mid- and late gastrula stage (Fig. 4). *foxY3* expression was enriched in clusters MG3, MG6 and MG8, which correspond to the archenteron and gut region (Fig. S6H,I). Furthermore, we detected *foxY3* and *vasa* co-expression at mid-gastrula using scRNA-seq (Fig. S7B). *wnt3* was also expressed in

Development (2022) 149, dev200982. doi:10.1242/dev.200982

the *vasa*, *foxY3*-positive cells, along with *wnt16* and *wnt1*; *wnt8* and *wnt3* were expressed in the cells neighboring the *vasa*, *foxY3*-positive cells (Fig. S7C; Table S5). This suggests differential expression of Wnt ligands in cells of the mid/hindgut region. Moreover, at this stage, *vasa*-positive cells expressed hindgut identity genes such as *gataE* and *foxA*, and the homeobox gene *hox11/13b* (*hbox7*) (Table S3; Fig. S7D). These findings are of particular importance for understanding how the germ line is formed, and would be difficult to ascertain using only *in situ* hybridization.

At the sea star mid-gastrula stage, the *vasa* transcript is expressed more broadly than in the future germ line. This contrasts its expression in the sea urchin, where it is restricted to the small micromeres in gastrulae, and in the mouse, where it is expressed only after the PGCs have colonized the embryonic gonad (Fujiwara et al., 1994; Juliano et al., 2006). This is a distinct strategy of cell-specific germ cell factor accumulation in which expression is spread broadly and then cleared from cells to yield highly localized expression. In the sea star, Vasa protein is also under strict control through selective post-translational degradation by Gustavus (Gus), an E3 ligase (Perillo et al., 2022). In the future, investigating how Nanos protein localization is regulated will inform us whether these transcripts are also under distinct regulation at the protein level. Here, we report co-expression of *vasa*-positive cells with the *foxY3* transcription factor. We also note Wnt ligand expression in *vasa*-positive cells and in cells of the same cluster identity that do not show *vasa* expression. We hypothesize that both Wnt and Delta/Notch signaling may regulate nanos and *vasa* expression at gastrula stage. These pathways could be active concurrently with Nodal restriction, which originates from a gradient on the right side of the embryo.

Echinoderms also offer an opportunity to investigate two modes of germ cell development in closely related species and uncover evolutionary differences. Nanos and Vasa eventually localize to putative PGC precursors in both species (the small micromeres in sea urchins and in the PE in the sea star), yet their embryonic expression patterns are vastly different. Early in sea urchin embryogenesis, nanos and *vasa* expression is restricted to the small micromeres (Juliano et al., 2006). In the sea urchin, nanos transcription is regulated by direct action of β-catenin in the small micromeres or the Delta/Notch transcription factor, FoxY, in the adjacent somatic Veg2 mesoderm cells (Oulhen et al., 2019). Whether canonical Wnt signaling plays a role in activating expression of nanos and *vasa* in sea star, and whether the *foxY3* transcription factor co-expressed with the germ line genes in sea star regulates their expression, could point to a regulatory node conserved between both species. Notably, in sea urchin, removal of the micromeres, the parent cells of the small micromeres, results in adults with developed gametes (Yajima and Wessel, 2011). Whether nanos expression, downstream of FoxY, in the Veg2 cells plays a role in reconstituting the germ line remains an interesting question and could point to an auxiliary, inductive mechanism present in the sea urchin. Testing effects of cell signaling perturbation in micromere-deleted embryos will help to decipher this process.

### Further cell type comparisons between species by scRNA-seq mechanisms

In the future, comparison of scRNA-seq datasets of different echinoderm species will likely reveal species-specific cell type differences. For example, at early blastula stage in the sea urchin, unique skeleton and pigment cell states are identified (Foster et al., 2020). Of note, the skeletogenic and pigment cell lineages are mesodermal cell types of the sea urchin, absent in the sea star embryo. However, here we report expression of *gcm*, a marker for pigment, and co-expression of *fos* and *mt1-4* markers expressed in primary mesenchyme cells present in sea urchin and not sea star embryos. Multi-species comparison could further reveal both similarities and differences between the transcriptomic profile of similar cell states between sea urchin and sea star.

The sea star (*P. miniata*) and sea urchin (*Paracentrotus lividus*) have been compared to assess heterochronies in marker gene expression, revealing a later onset of maternal to embryonic transition in the sea star compared with this sea urchin (Gildor et al., 2017). It is possible that this temporal difference plays a role in the diversity of cell states present or differences in lineage mapping of early developmental stages when comparing two species. An alternative hypothesis is that cell fates in the sea star rely more on cell signaling for fate decisions than in the sea urchin, and that this difference is revealed by scRNA-seq analysis.

### Evolution of germ line specification

Evidence suggests that the inductive mode (epigenesis) in metazoans, such as sponges, jellyfish and hydra, is the ancestral mechanism of germ cell specification (Extavour and Akam, 2003). Discovery of an inductive mode for germ line specification in the sea star, an echinoderm species, presents an opportunity for comparative analysis with the mouse, a mammalian species for which we have the most comprehensive description of the inductive mechanism. Mouse PGCs acquire their fate in response to signaling and arise from mesoderm differentiating cells. Single-cell analysis revealed that early germ cells express homeobox genes, including *Hoxb1* and *Hoxa1*, and the mesodermal marker brachyury (*T*), at the same level as their somatic cell neighbors. The early germ cells then initiate transcriptional repression of homeobox genes, which remain highly expressed in the neighboring somatic cells as the embryo develops (Saitou et al., 2003). Here, we see a similarity in the sea star, with co-expression of *hox11/13b* and *brachyury* with nanos-positive cells (Fig. S7D). In the mouse, expression of germline determinants with mesodermal markers is resolved by repression of the mesodermal markers in the PGC precursor cells; *Stella* (*Dppa3*)-positive cells repress homeobox genes (Saitou et al., 2003). Cell lineage analysis of scRNA-seq data in mice also reveals a lack of germ cell determinants in somatic cells and vice versa (Chan et al., 2019). Notably, the axolotl homologue of *brachyury*, a well conserved mesodermal marker, *Axbra*, is seen in all cells of the mesodermal region known to include PGC precursors, suggesting that the PGC precursors express *brachyury* and are specified from early mesoderm (Johnson et al., 2003). If and how expression of mesodermal markers such as brachyury affects germ cell development in mice, axolotls and sea stars may reveal whether there is a conserved relationship between mesodermal and germ cell factor expression in inductive germ line specification mechanisms. Thus, in the sea star, apart from restricting nanos and *vasa* transcript expression, repression of mesodermal markers in nanos- and *vasa*-positive cells remains an important step in germ line specification, which has yet to be identified.

## MATERIALS AND METHODS

### Embryo culture and dissociation for single cell analysis

Adult *P. miniata* animals were collected by either Peter Halmay (San Diego Fishermen's Working Group) or Josh Ross (South Coast Bio-Marine) off the Californian coast. Embryos were cultured essentially as described previously (Fresques et al., 2016). Embryos were cultured in filtered (0.2 µm) sea water collected at the Marine Biological Laboratories in Woods Hole, MA, USA, until the appropriate stage for dissociation. All embryos used in the study resulted from the mating of one male and one female to ensure complete comparative capability. Multiple fertilizations were

Development (2022) 149, dev200982. doi:10.1242/dev.200982

initiated in this study and timed such that the appropriate stages of embryonic development were reached at a common endpoint. The embryos were then collected and washed twice with calcium-free sea water, and then suspended in hyalin-extraction media (HEM) for 10-15 min, depending on the stage of dissociation. When cells were beginning to dissociate, the embryos were collected and washed in 0.5 M NaCl, gently sheared with a pipette, run through a 40 µm Nitex mesh, counted on a hemocytometer and diluted to reach the appropriate concentration for the scRNA-seq protocol. Equal numbers of embryos were used in each time point and at no time were cells or embryos pelleted in a centrifuge (Oulhen et al., 2019).

### *In situ* hybridization

DIG-labeled RNA probes were made using a Roche DIG probe synthesis kit as described previously (Fresques et al., 2016). Probe-hybridized embryos were developed with NBT+BCIP for purple staining. Embryos were incubated with a probe for 1 week and were developed essentially as described previously (Fresques et al., 2016).

### scRNA-seq

Single cell encapsulation was performed using the Chromium Single Cell Chip B kit on the 10x Genomics Chromium Controller. Single cell cDNA and libraries were prepared using the Chromium Single Cell 3′ Reagent kit v3 Chemistry. Libraries were sequenced by Genewiz on the Illumina Hiseq (2×150 bp paired-end runs). Single-cell unique molecular identifier (Fujii et al., 2009) counting (counting of unique barcodes given to individual transcript molecules) was performed using Cell Ranger Single Cell Software Suite 3.0.2 from 10x Genomics. The custom transcriptome reference was generated from *P. miniata* assembly V2.0 (echinobase.org) using CellRanger mkref. The *P. miniata* V2.0 assembly was used for analysis owing to a higher rate of genome mapping compared with V3.0. In addition, the germ line genes analyzed in this study are annotated in V2.0. The annotation for *Pm*-nanos was manually edited to account for a longer 3′ untranslated region. Duplicate blastula and gastrula stage libraries were aggregated using the cellranger aggr function. Cellranger gene expression matrices were further analyzed using the R package Seurat v 3.2.2 (Stuart et al., 2019). Cells of 8-14 hpf stages with at least 1000 and at most 6000 genes (features), and cells with at least 1000 and at most 2500 genes in blastula to mid-gastrula stages were included in downstream analysis. Individual datasets were normalized by scaling gene expression in each cell by total gene expression and then log transformed. The top 2000 highly variable genes across the datasets were then used to integrate the datasets. Individual time point datasets were integrated using the Seurat toolkit Harmony to remove batch effects and identify conserved cell populations across the datasets. The clustering parameters used were: dimensions, 20; resolution, 1.0. Cluster markers were found using FindConservedMarkers and FindMarkers functions. The UMI count and gene number per cell are presented in Figs S8 and S9. See Supplementary Data 1 for the code used (PmAnalysis.txt).

#### Acknowledgements

Part of this research was conducted using resources and services at the Computational Biology Core and Center for Computation and Visualization, Brown University. A special thanks to August Guang, Joselynn Wallace and Ashok Ragavendran of the Computational Biology Core.

#### Competing interests

The authors declare no competing or financial interests.

#### Author contributions

Conceptualization: S.F., N.O., T.F., G.W.; Methodology: S.F., N.O., H.Z.; Validation: S.F., N.O., G.W.; Formal analysis: S.F., N.O., H.Z.; Investigation: S.F., N.O., T.F.; Resources: G.W.; Data curation: S.F., N.O.; Writing - review & editing: S.F., N.O., T.F., G.W.; Visualization: N.O., T.F., H.Z.; Supervision: G.W.; Project administration: G.W.; Funding acquisition: G.W.

#### Funding

We thank the National Institutes of Health (1R35GM140897, G.W. and 1P20GM119943, N.O.) and the National Science Foundation (IOS-1923445, G.W.). Deposited in PMC for release after 12 months.

#### Data availability

Datasets have been deposited in GEO under accession number GSE196654.

#### References

**Annunziata, R., Martinez, P. and Arnone, M. I.** (2013). Intact cluster and chordate-like expression of ParaHox genes in a sea star. *BMC Biol.* **11**, 68. doi:10.1186/1741-7007-11-68

**Briggs, J. A., Weinreb, C., Wagner, D. E., Megason, S., Peshkin, L., Kirschner, M. W. and Klein, A. M.** (2018). The dynamics of gene expression in vertebrate embryogenesis at single-cell resolution. *Science* **360**, eaar5780. doi:10.1126/science.aar5780

**Calestani, C., Rast, J. P. and Davidson, E. H.** (2003). Isolation of pigment cell specific genes in the sea urchin embryo by differential macroarray screening. *Development* **130**, 4587-4596. doi:10.1242/dev.00647

**Cary, G. A., Mccauley, B. S., Zueva, O., Pattinato, J., Longabaugh, W. and Hinman, V. F.** (2020). Systematic comparison of sea urchin and sea star developmental gene regulatory networks explains how novelty is incorporated in early development. *Nat. Commun.* **11**, 6235. doi:10.1038/s41467-020-20023-4

**Chan, M. M., Smith, Z. D., Grosswendt, S., Kretzmer, H., Norman, T. M., Adamson, B., Jost, M., Quinn, J. J., Yang, D., Jones, M. G. et al.** (2019). Molecular recording of mammalian embryogenesis. *Nature* **570**, 77-82. doi:10.1038/s41586-019-1184-5

**Cheatle Jarvela, A. M., Yankura, K. A. and Hinman, V. F.** (2016). A gene regulatory network for apical organ neurogenesis and its spatial control in sea star embryos. *Development* **143**, 4214-4223. doi:10.1242/dev.134999

**Davidson, E. H.** (2006). *The Regulatory Genome*. San Diego: Academic Press.

**Duboc, V., Rottinger, E., Lapraz, F., Besnardeau, L. and Lepage, T.** (2005). Left-right asymmetry in the sea urchin embryo is regulated by nodal signaling on the right side. *Dev. Cell* **9**, 147-158. doi:10.1016/j.devcel.2005.05.008

**Extavour, C. G. and Akam, M.** (2003). Mechanisms of germ cell specification across the metazoans: epigenesis and preformation. *Development* **130**, 5869-5884. doi:10.1242/dev.00804

**Foster, S., Oulhen, N. and Wessel, G.** (2020). A single cell RNA sequencing resource for early sea urchin development. *Development* **147**, dev191528. doi:10.1242/dev.191528

**Fresques, T. M. and Wessel, G. M.** (2018). Nodal induces sequential restriction of germ cell factors during primordial germ cell specification. *Development* **145**, dev155663. doi:10.1242/dev.155663

**Fresques, T., Zazueta-Novoa, V., Reich, A. and Wessel, G. M.** (2014). Selective accumulation of germ-line associated gene products in early development of the sea star and distinct differences from germ-line development in the sea urchin. *Dev. Dyn.* **243**, 568-587. doi:10.1002/dvdy.24038

**Fresques, T., Swartz, S. Z., Juliano, C., Morino, Y., Kikuchi, M., Akasaka, K., Wada, H., Yajima, M. and Wessel, G. M.** (2016). The diversity of nanos expression in echinoderm embryos supports different mechanisms in germ cell specification. *Evol. Dev.* **18**, 267-278. doi:10.1111/ede.12197

**Fujii, T., Sakamoto, N., Ochiai, H., Fujita, K., Okamitsu, Y., Sumiyoshi, N., Minokawa, T. and Yamamoto, T.** (2009). Role of the nanos homolog during sea urchin development. *Dev. Dyn.* **238**, 2511-2521. doi:10.1002/dvdy.22074

**Fujiwara, Y., Komiya, T., Kawabata, H., Sato, M., Fujimoto, H., Furusawa, M. and Noce, T.** (1994). Isolation of a DEAD-family protein gene that encodes a murine homolog of Drosophila vasa and its specific expression in germ cell lineage. *Proc. Natl. Acad. Sci. USA* **91**, 12258-12262. doi:10.1073/pnas.91.25.12258

**Gildor, T., Hinman, V. and Ben-Tabou-De-Leon, S.** (2017). Regulatory heterochronies and loose temporal scaling between sea star and sea urchin regulatory circuits. *Int. J. Dev. Biol.* **61**, 347-356. doi:10.1387/ijdb.160331sb

**Hibino, T., Loza-Coll, M., Messier, C., Majeske, A. J., Cohen, A. H., Terwilliger, D. P., Buckley, K. M., Brockton, V., Nair, S. V., Berney, K. et al.** (2006). The immune gene repertoire encoded in the purple sea urchin genome. *Dev. Biol.* **300**, 349-365. doi:10.1016/j.ydbio.2006.08.065

**Hinman, V. F. and Burke, R. D.** (2018). Embryonic neurogenesis in echinoderms. *Wiley Interdiscip. Rev. Dev. Biol.* **7**, e316. doi:10.1002/wdev.316

**Hinman, V. F. and Davidson, E. H.** (2003). Expression of a gene encoding a Gata transcription factor during embryogenesis of the starfish Asterina miniata. *Gene Expr. Patterns* **3**, 419-422. doi:10.1016/S1567-133X(03)00082-6

**Hinman, V. F. and Davidson, E. H.** (2007). Evolutionary plasticity of developmental gene regulatory network architecture. *Proc. Natl. Acad. Sci. USA* **104**, 19404-19409. doi:10.1073/pnas.0709994104

**Hinman, V. F., Nguyen, A. T., Cameron, R. A. and Davidson, E. H.** (2003). Developmental gene regulatory network architecture across 500 million years of echinoderm evolution. *Proc. Natl. Acad. Sci. USA* **100**, 13356-13361. doi:10.1073/pnas.2235868100

**Inoue, C., Kiyomoto, M. and Shirai, H.** (1992). Germ cell differentiation in starfish: the posterior enterocoel as the origin of germ cells in Asterina pectinifera. *Dev. Growth Differ.* **34**, 413-418. doi:10.1111/j.1440-169X.1992.00413.x

**Johnson, A. D., Crother, B., White, M. E., Patient, R., Bachvarova, R. F., Drum, M. and Masi, T.** (2003). Regulative germ cell specification in axolotl embryos: a primitive trait conserved in the mammalian lineage. *Philos. Trans. R. Soc. Lond. B Biol. Sci.* **358**, 1371-1379. doi:10.1098/rstb.2003.1331

**Juliano, C. E., Voronina, E., Stack, C., Aldrich, M., Cameron, A. R. and Wessel, G. M.** (2006). Germ line determinants are not localized early in sea urchin development, but do accumulate in the small micromere lineage. *Dev. Biol.* **300**, 406-415. doi:10.1016/j.ydbio.2006.07.035

**Korsunsky, I., Millard, N., Fan, J., Slowikowski, K., Zhang, F., Wei, K., Baglaenko, Y., Brenner, M., Loh, P. R. and Raychaudhuri, S.** (2019). Fast, sensitive and accurate integration of single-cell data with Harmony. *Nat. Methods* **16**, 1289-1296. doi:10.1038/s41592-019-0619-0

**Macosko, E. Z., Basu, A., Satija, R., Nemesh, J., Shekhar, K., Goldman, M., Tirosh, I., Bialas, A. R., Kamitaki, N., Martersteck, E. M. et al.** (2015). Highly parallel genome-wide expression profiling of individual cells using nanoliter droplets. *Cell* **161**, 1202-1214. doi:10.1016/j.cell.2015.05.002

**Massri, A. J., Greenstreet, L., Afanassiev, A., Berrio, A., Wray, G. A., Schiebinger, G. and Mcclay, D. R.** (2021). Developmental single-cell transcriptomics in the Lytechinus variegatus sea urchin embryo. *Development* **148**, dev198614. doi:10.1242/dev.198614

**Materna, S. C., Swartz, S. Z. and Smith, J.** (2013). Notch and Nodal control forkhead factor expression in the specification of multipotent progenitors in sea urchin. *Development* **140**, 1796-1806. doi:10.1242/dev.091157

**Mccauley, B. S., Weideman, E. P. and Hinman, V. F.** (2010). A conserved gene regulatory network subcircuit drives different developmental fates in the vegetal pole of highly divergent echinoderm embryos. *Dev. Biol.* **340**, 200-208. doi:10.1016/j.ydbio.2009.11.020

**Mccauley, B. S., Akyar, E., Filliger, L. and Hinman, V. F.** (2013). Expression of wnt and frizzled genes during early sea star development. *Gene Expr. Patterns* **13**, 437-444. doi:10.1016/j.gep.2013.07.007

**Nishihira, J.** (2000). Macrophage migration inhibitory factor (MIF): its essential role in the immune system and cell growth. *J. Interferon Cytokine Res.* **20**, 751-762. doi:10.1089/10799900050151012

**Oulhen, N., Swartz, S. Z., Wang, L., Wikramanayake, A. and Wessel, G. M.** (2019). Distinct transcriptional regulation of Nanos2 in the germ line and soma by the Wnt and delta/notch pathways. *Dev. Biol.* **452**, 34-42. doi:10.1016/j.ydbio.2019.04.010

**Paganos, P., Voronov, D., Musser, J. M., Arendt, D. and Arnone, M. I.** (2021). Single-cell RNA sequencing of the Strongylocentrotus purpuratus larva reveals the blueprint of major cell types and nervous system of a non-chordate deuterostome. *Elife* **10**, e70416. doi:10.7554/eLife.70416

**Perillo, M., Swartz, S. Z. and Wessel, G. M.** (2022). A conserved node in the regulation of Vasa between an induced and an inherited program of primordial germ cell specification. *Dev. Biol.* **482**, 28-33. doi:10.1016/j.ydbio.2021.11.007

**Rafiq, K., Cheers, M. S. and Ettensohn, C. A.** (2012). The genomic regulatory control of skeletal morphogenesis in the sea urchin. *Development* **139**, 579-590. doi:10.1242/dev.073049

**Saitou, M., Payer, B., Lange, U. C., Erhardt, S., Barton, S. C. and Surani, M. A.** (2003). Specification of germ cell fate in mice. *Philos. Trans. R. Soc. Lond. B Biol. Sci.* **358**, 1363-1370. doi:10.1098/rstb.2003.1324

**Stuart, T., Butler, A., Hoffman, P., Hafemeister, C., Papalexi, E., Mauck, W. M., III, Hao, Y., Stoeckius, M., Smibert, P. and Satija, R**. (2019). Comprehensive integration of single-cell data. *Cell* **177**, 1888-1902. doi:10.1016/j.cell.2019.05.031

**Sun, Z. and Ettensohn, C. A.** (2014). Signal-dependent regulation of the sea urchin skeletogenic gene regulatory network. *Gene Expr. Patterns* **16**, 93-103. doi:10.1016/j.gep.2014.10.002

**Yajima, M. and Wessel, G. M.** (2011). Small micromeres contribute to the germline in the sea urchin. *Development* **138**, 237-243. doi:10.1242/dev.054940

**Yankura, K. A., Koechlein, C. S., Cryan, A. F., Cheatle, A. and Hinman, V. F.** (2013). Gene regulatory network for neurogenesis in a sea star embryo connects broad neural specification and localized patterning. *Proc. Natl. Acad. Sci. USA* **110**, 8591-8596. doi:10.1073/pnas.1220903110

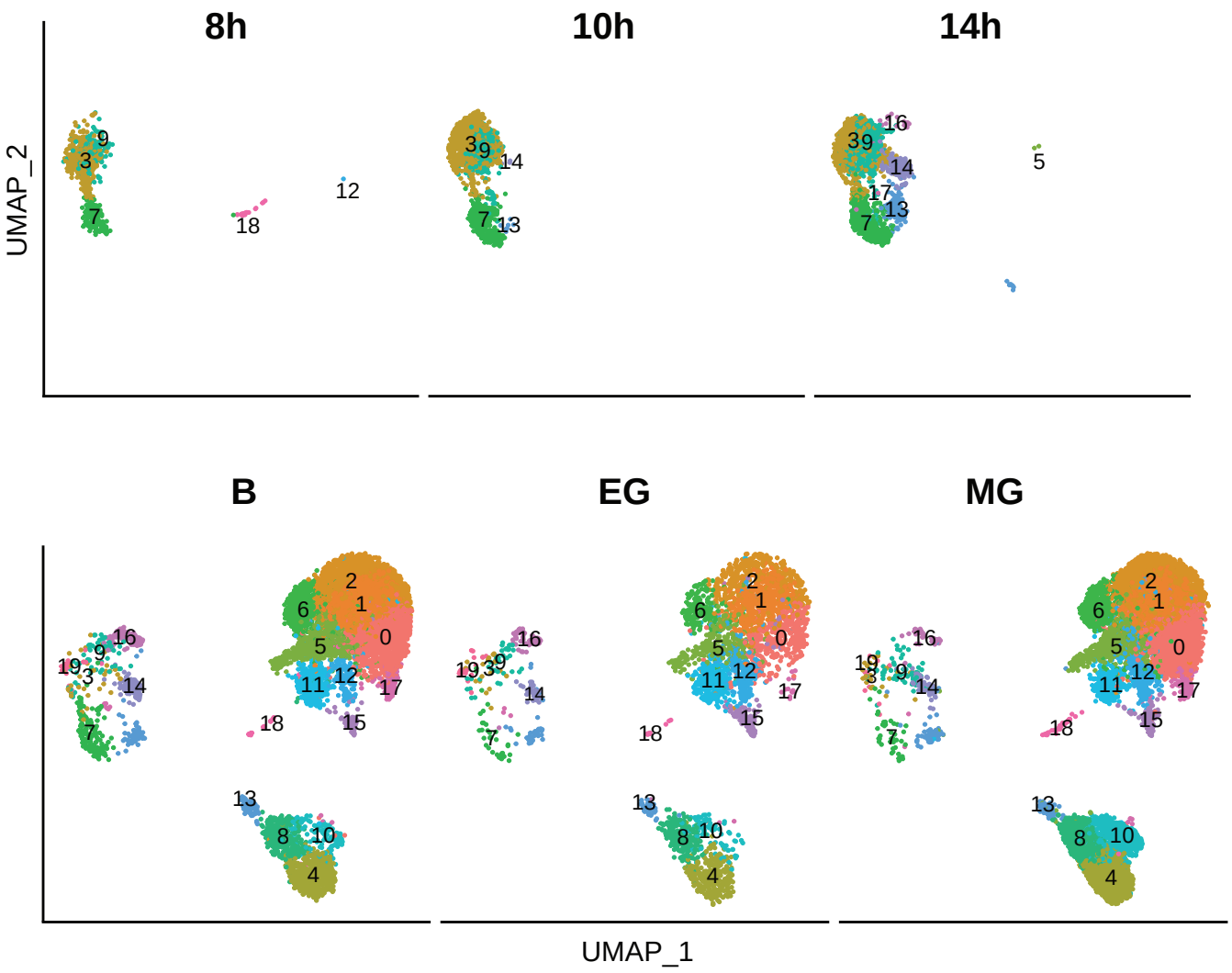


**Fig. S1. Identification of cell states across early sea star development.** UMAP visualization of six integrated datasets, separated by embryonic stage: 8-hpf (868 cells), 10-hpf (1,318 cells), 14-hpf (2,448 cells), blastula (7,272 cells), early gastrula (3,349 cells), and mid-gastrula (10,448 cells).

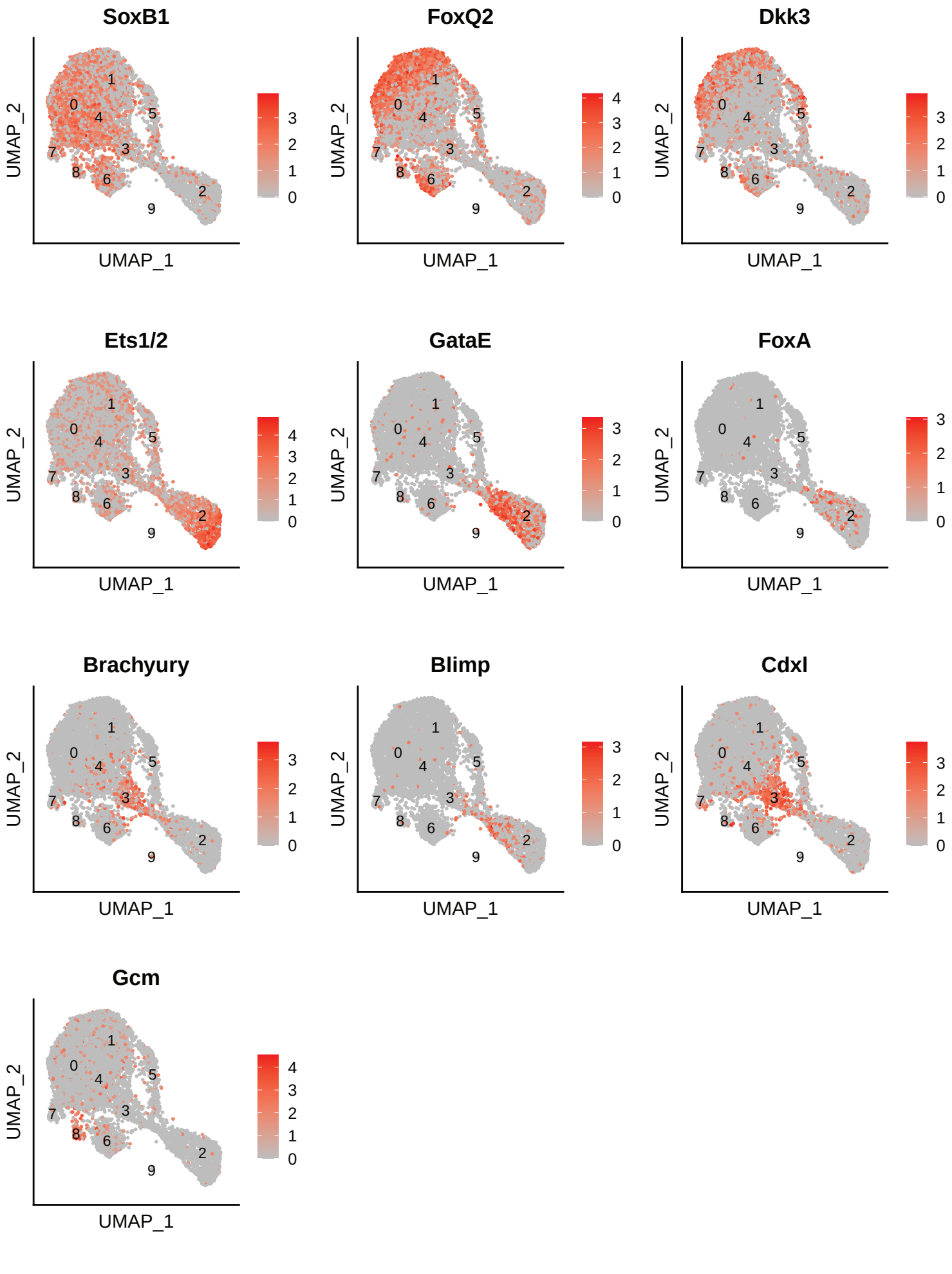


**Fig. S2. Marker gene expression at blastula stage.** Feature plotsshowing expression of ectodermal, mesodermal, and endodermal marker genes at blastula stage. Average gene expression level displayed by color intensity.

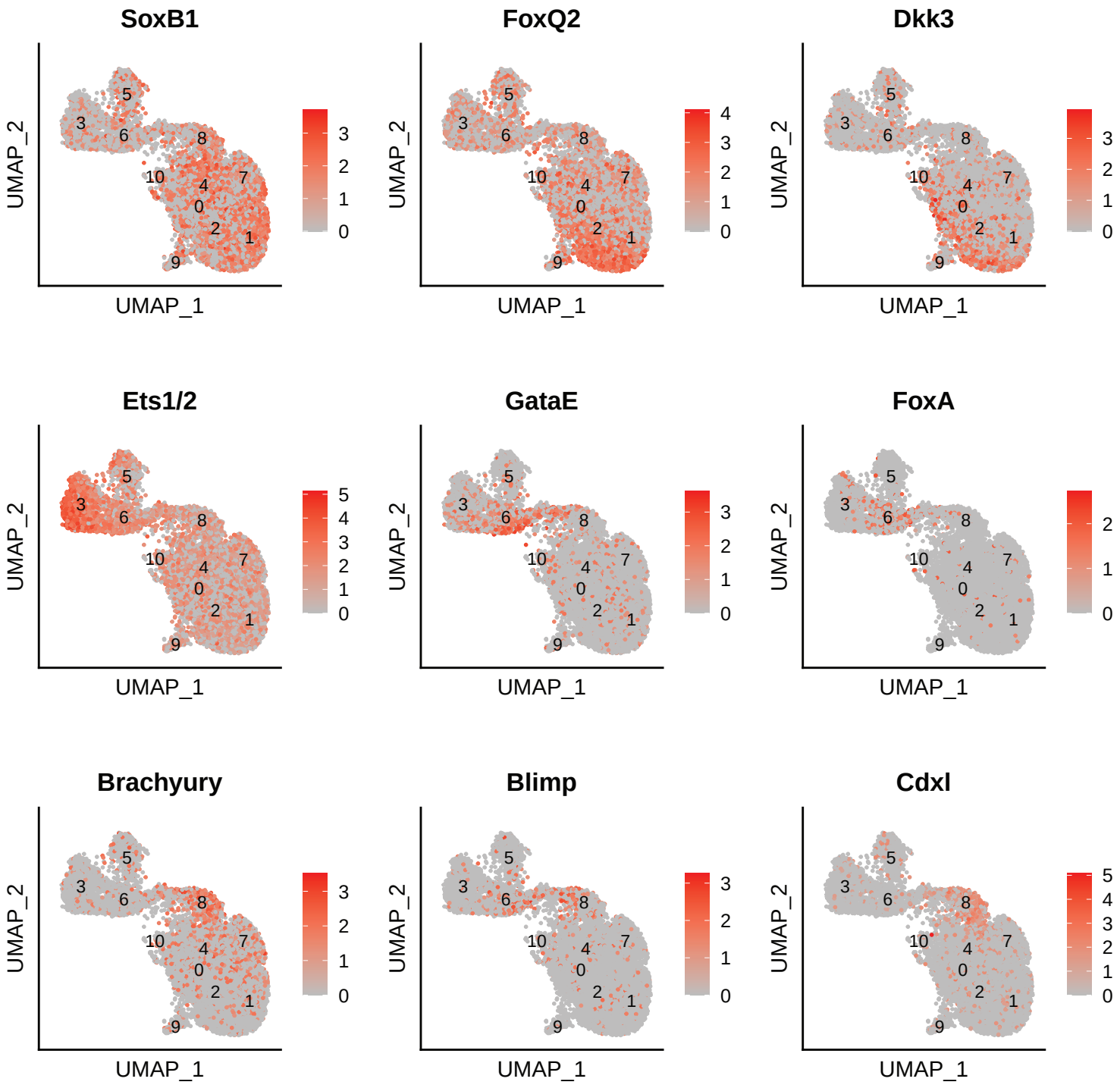


**Fig. S3. Marker gene expression at mid-gastrula stage.** Featureplots showing expression of ectodermal, mesodermal, and endodermal marker genes atmid-gastrula stage. Average gene expression level displayed by color intensity.

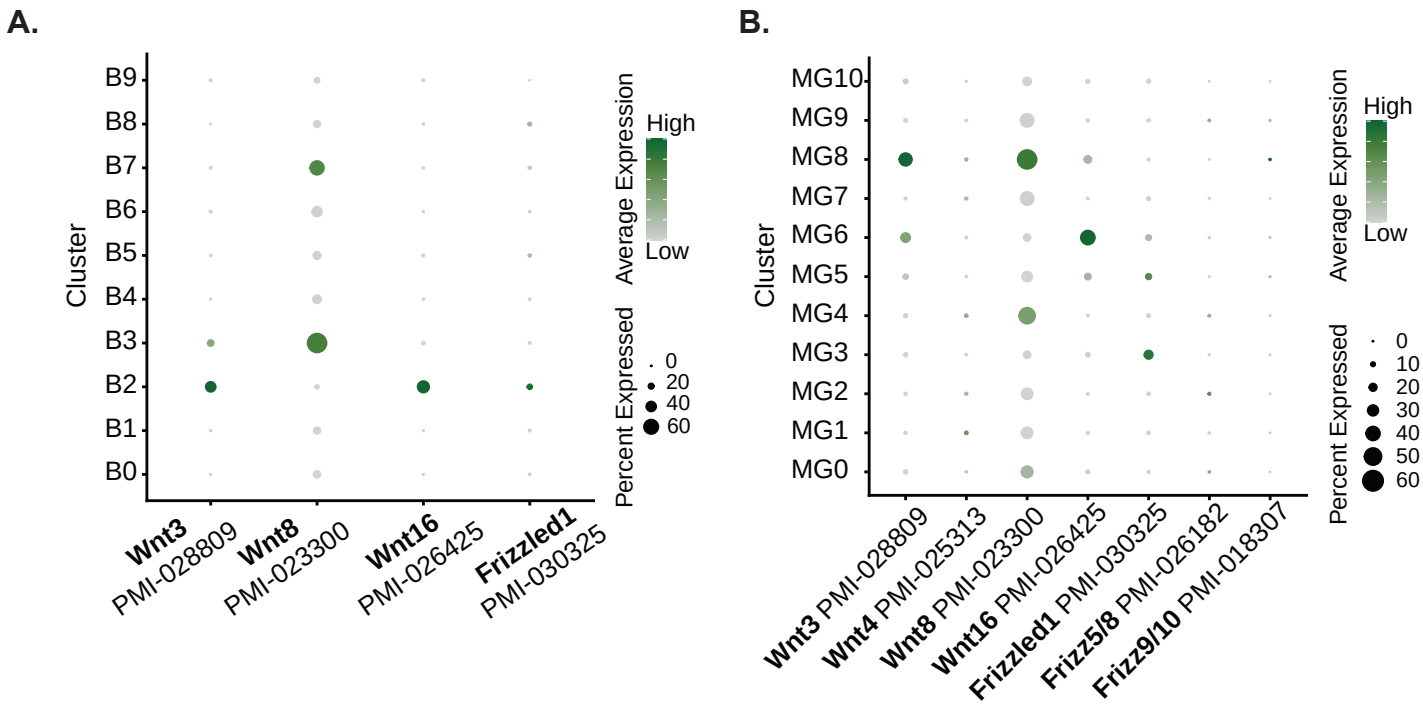


**Fig. S4. Wnt signaling component expression.** (A) Dot plot of Wntsignaling pathway component expression at blastula stage. Co-expression of Wnt3, Wnt16, and Frizzled1 receptor (Annotated as Frizz in the dataset) seen in cluster B2. (B) Dot plot of Wnt signaling pathway component expression at mid-gastrula stage.

**A.**

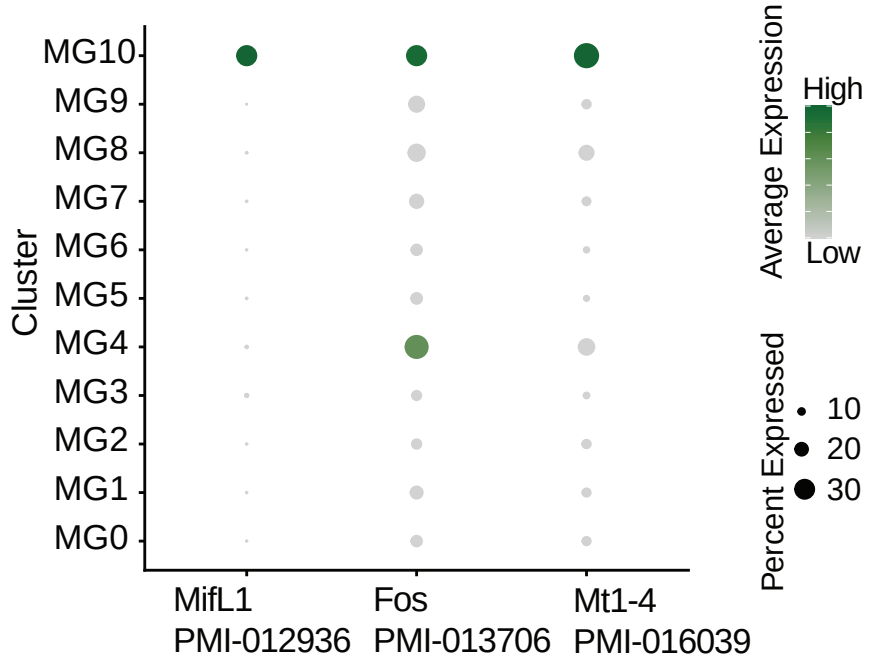


**B.**

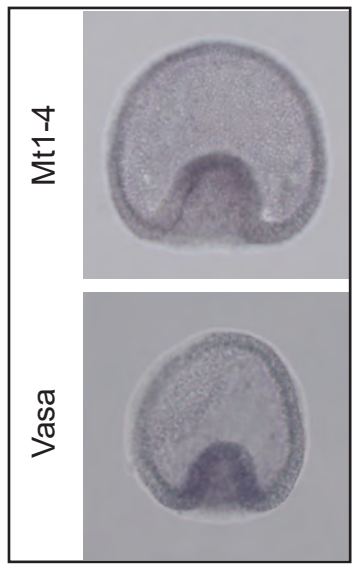


**Fig. S5. MifL1-enriched cluster expression.** (A) Dot plot showingexpression of sea urchin PMC marker genes Mt1-4 and Fos in cluster 10, MifL1- enriched cluster, at mid-gastrula stage. (B) Whole mount in situ hybridizations for Mt1-4 and Vasa in sea star gastrulae.

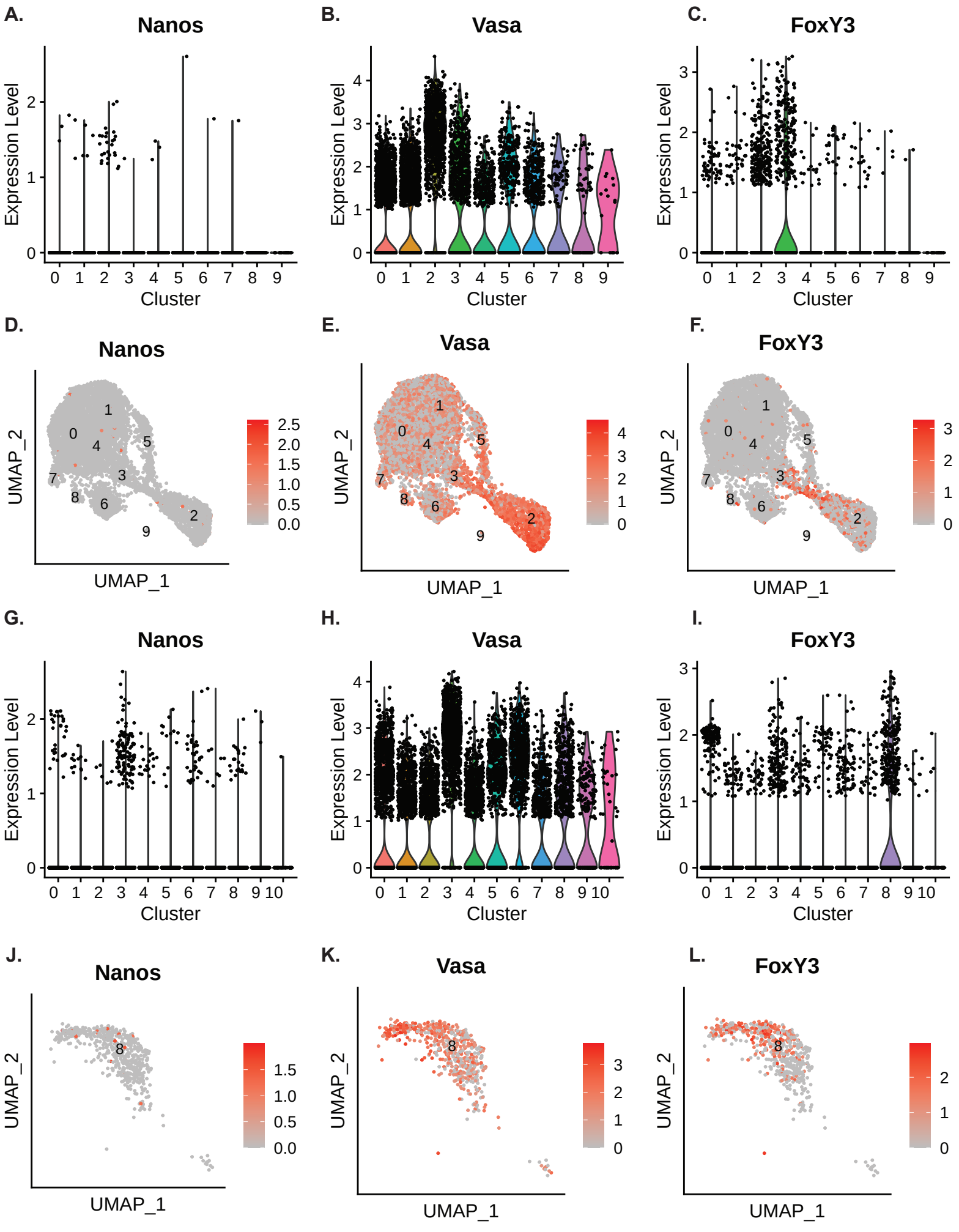
A.
Nanos
Expression Level
Cluster
B.
Vasa
Expression Level
Cluster
C.
FoxY3
Expression Level
Cluster
D.
Nanos
UMAP_2
UMAP_1
E.
Vasa
UMAP_2
UMAP_1
F.
FoxY3
UMAP_2
UMAP_1
G.
Nanos
Expression Level
Cluster
H.
Vasa
Expression Level
Cluster
I.
FoxY3
Expression Level
Cluster
J.
Nanos
UMAP_2
UMAP_1
K.
Vasa
UMAP_2
UMAP_1
L.
FoxY3
UMAP_2
UMAP_1

**Fig. S6. Vasa, Nanos, and FoxY3 expression.** Violin plots showing Nanos, Vasa, and FoxY3 expression per cluster in blastula stage (Hibino et al.) and mid-gastrula stage (G-I). Feature plots showing expression of Nanos, Vasa, and FoxY3in blastula stage (D-F) and in cluster 8 of mid-gastrula stage (J-L).

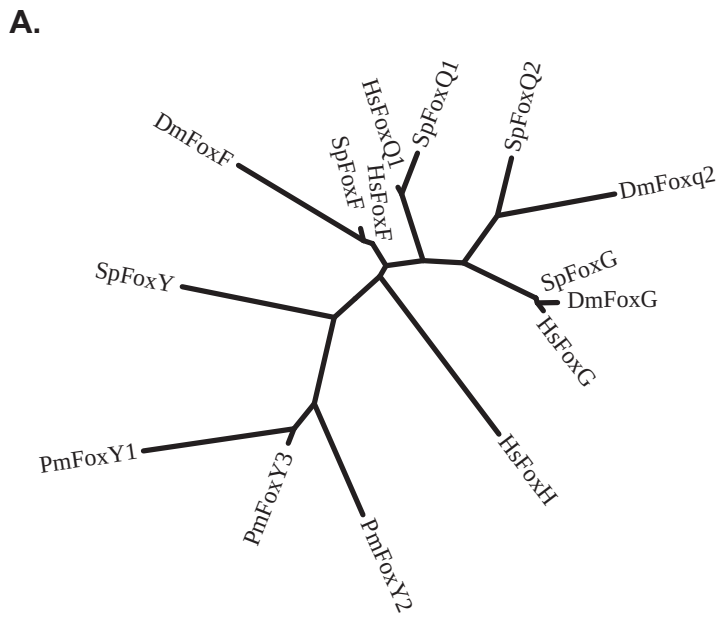
A.
DmFoxF
HsFoxQ1
SpFoxQ1
SpFoxQ2
SpFoxF
HsFoxF
DmFoxq2
SpFoxY
SpFoxG
DmFoxG
HsFoxG
PmFoxY1
PmFoxY3
HsFoxH
PmFoxY2

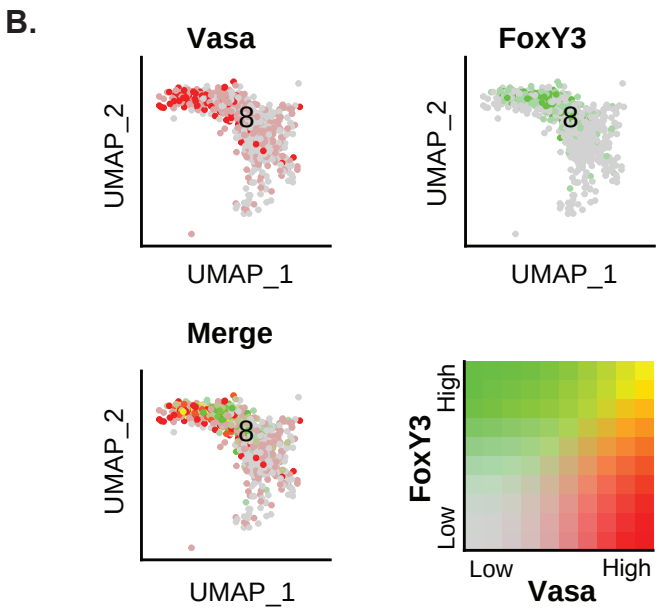
B.
Vasa
FoxY3
Merge
UMAP_2
UMAP_1
8
FoxY3
High
Low
Low
High
Vasa

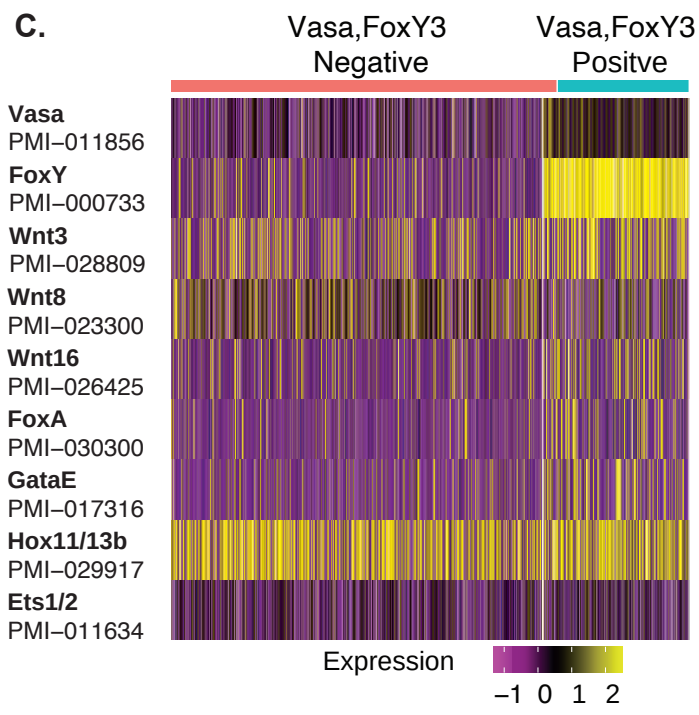
C.
Vasa,FoxY3 Negative
Vasa,FoxY3 Positve
Vasa
PMI–011856
FoxY
PMI–000733
Wnt3
PMI–028809
Wnt8
PMI–023300
Wnt16
PMI–026425
FoxA
PMI–030300
GataE
PMI–017316
Hox11/13b
PMI–029917
Ets1/2
PMI–011634
Expression
–1 0 1 2

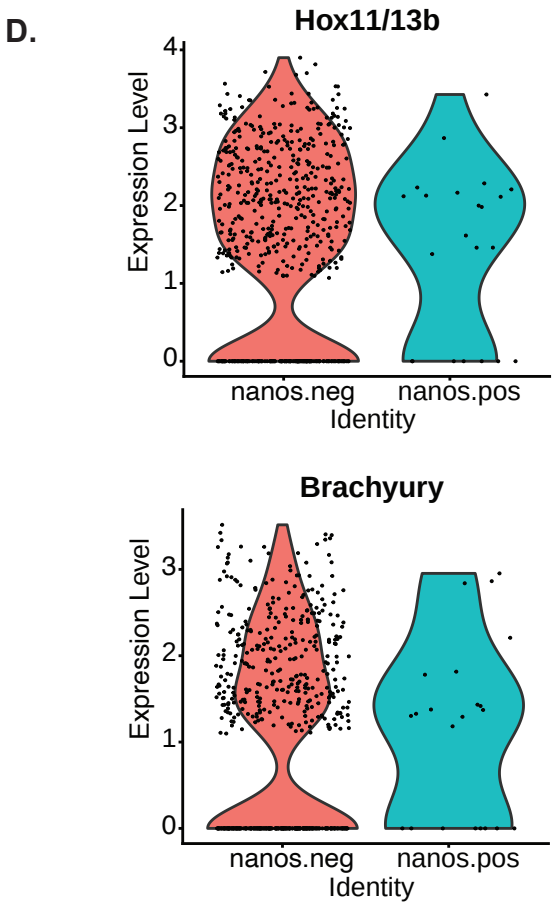
D.
Hox11/13b
Expression Level
0
1
2
3
4
nanos.neg
nanos.pos
Identity
Brachyury
Expression Level
0
1
2
3
nanos.neg
nanos.pos
Identity

**Fig. S7. Vasa and FoxY3 expression.** (A) Phylogenetic tree of FoxY transcription factors. Pm (*Patiria miniata*), Sp (*Strongylocentrotus purpuratus*), Dm (*Drosophila melanogaster*), Hs (*Homo sapiens*). FoxY3 (PMI_000733), previously annotated as FoxQ1, was found to be most similar to SpFoxY based on multiple protein sequence alignment. FoxY1 (PMI_028394). FoxY2 (PMI_008472). (B) Vasa expression in 395 cells of mid-gastrula cluster 8 (hindgut) shown in red (top left). FoxY3 expression in 221 cellsof cluster 8 shown in green (top right). Merge showing co-expression of Vasa and FoxY3 in 167 cells (bottom left). Color scale for expression level (bottom right). (C) Heatmap comparing expression in cells co-expressing Vasa and FoxY3 to those that donot co-express Vasa and FoxY3 in cells of cluster 8 of mid-gastrula stage (hindgut). (D) Violin plot of Hox11/13b and Brachyury expression in Nanos negative and Nanos positive cells of mid-gastrula cluster 8.

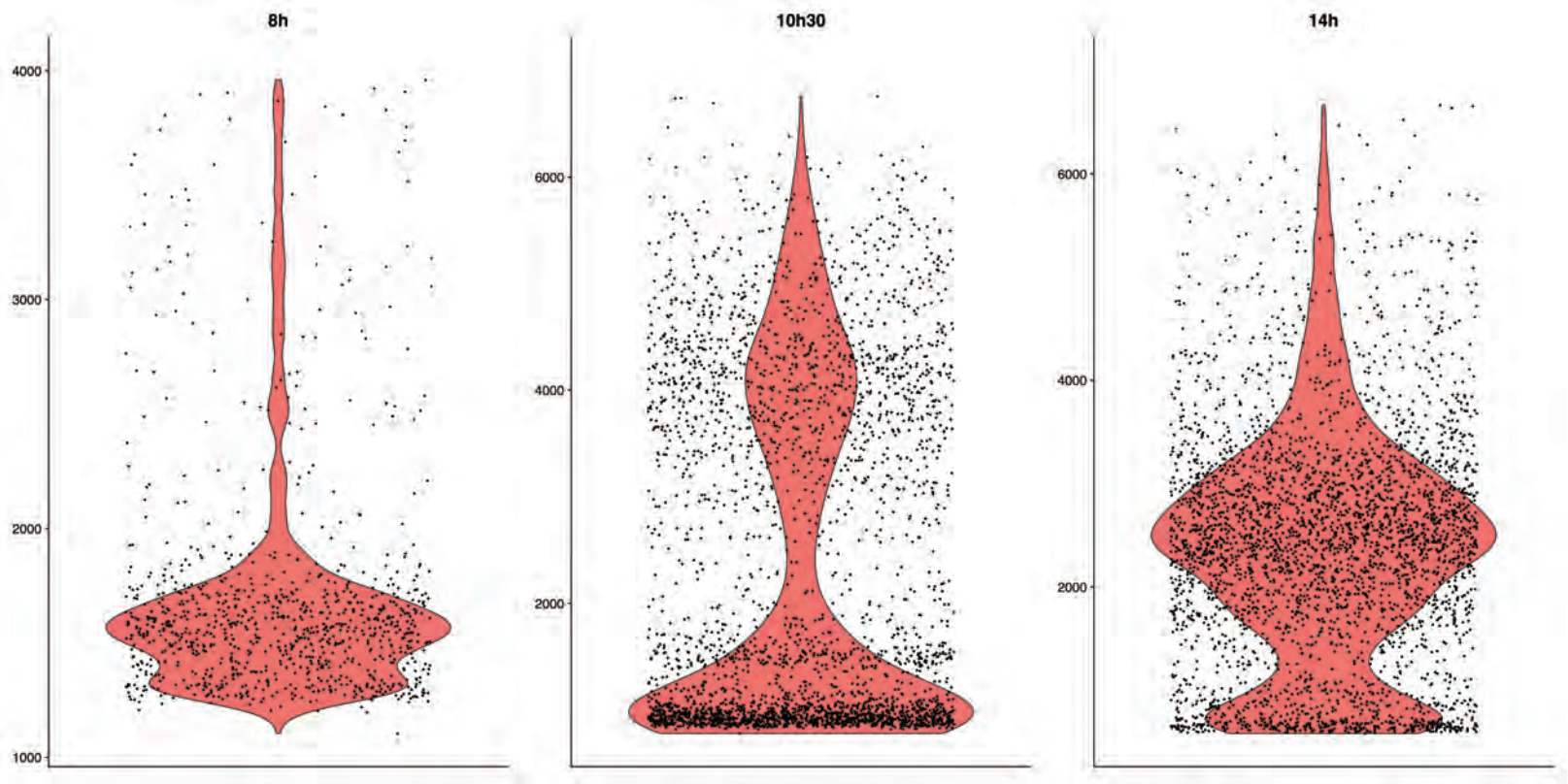


**Fig. S8. Total genes detected per cell across developmental time points.**

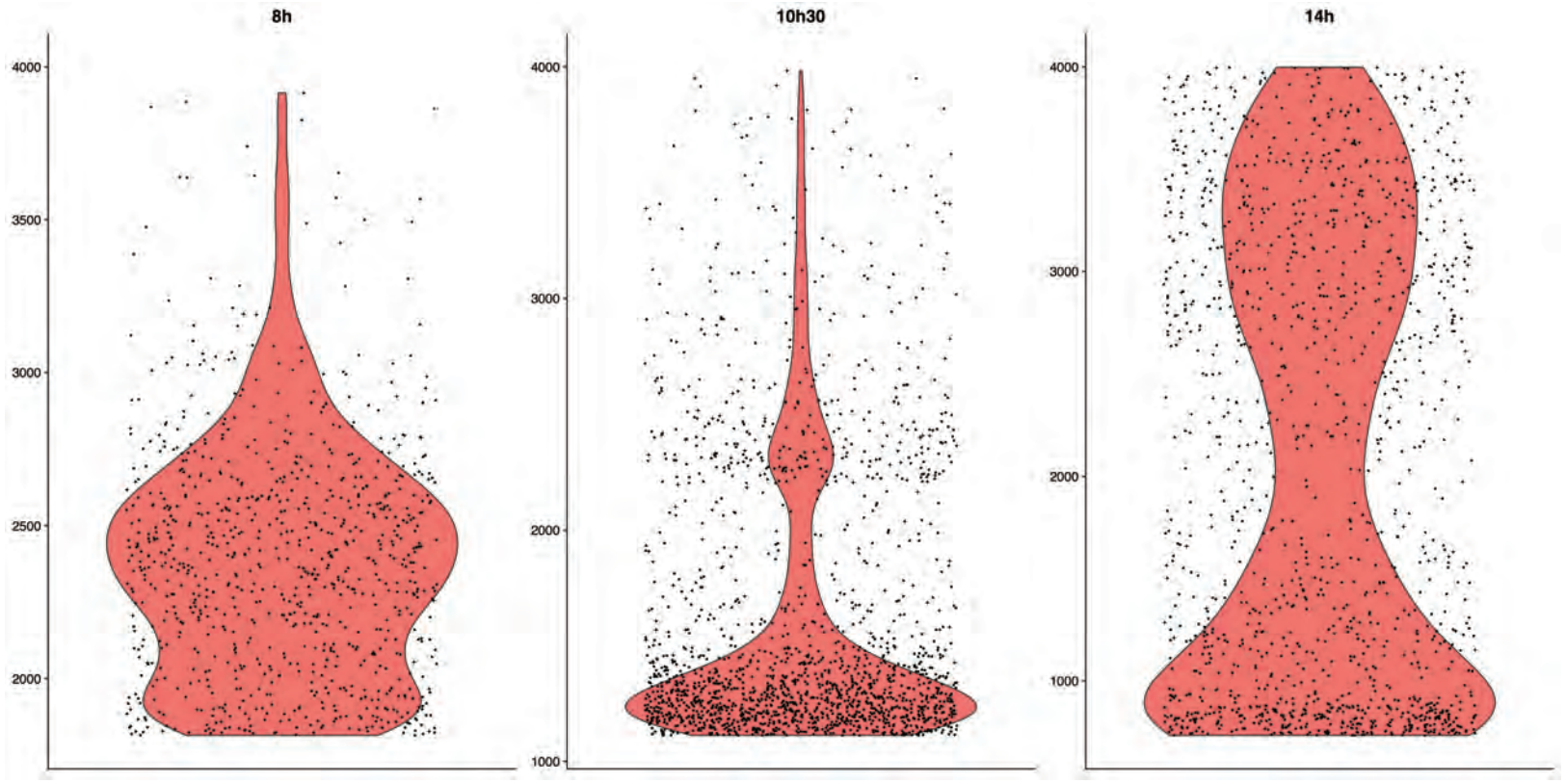


**Fig. S9. Total UMIs detected per cell across developmental time points.**

**Table S1. Blastula Stage** Cell State Identification and proportion of cells per cluster: 7,272 total cells

| | | **Marker gene** | **Number of cells** | **Percent of dataset** |
|---|---|---|---|---|
| Cluster 0 ● | Ectoderm: | SoxB1, Dkk3 | 2349 | 32.3 |
| Cluster 1 ● | Ectoderm: Apical, Neuronal | FoxQ2, DKK3, Syt14 (synaptotagmin) | 1528 | 21.0 |
| Cluster 2 ● | Presumptive mesoderm | Ets1/2, GataE, Tbr, Wnt16, | 1006 | 13.8 |
| Cluster 3 ● | Presumptive endoderm | Cdxl, Bra, Nk1, Wnt8, FoxY3 (annotated as Foxq1) | 695 | 9.5 |
| Cluster 4 ● | Ectoderm: Oral | Nodal, Lefty, Chordin, Bmp2/4 | 521 | 7.2 |
| Cluster 5 ● | Ectoderm: Apical pole | Dkk3, Hyalin | 489 | 6.7 |
| Cluster 6 ● | Ectoderm: Lateral | Wnt16, Nodal, Lefty | 455 | 6.2 |
| Cluster 7 ● | Ectoderm: Vegetal | Fos1, Mt1-4, Wnt8, Jun | 124 | 1.7 |
| Cluster 8 ● | Gcm enriched | Gcm, Delta | 87 | 1.2 |
| Cluster 9 ● | MifL1 enriched | MifL1, Mt1-4, Ets4 | 18 | 0.2 |

**Mid-Gastrula Stage** Cell State Identification and proportion of cells per cluster: 10,448 total cells

| | | **Marker gene** | **Number of cells** | **Percent of dataset** |
|---|---|---|---|---|
| Cluster 0 ● | Ectoderm | SoxB1 | 2407 | 23.0 |
| Cluster 1 ● | Ectoderm | SoxB1, FoxQ2 (PMI-009167 Nkx3.2) | 1437 | 13.7 |
| Cluster 2 ● | Ectoderm: Apical | Dkk3, FoxQ2 | 1193 | 11.4 |
| Cluster 3 ● | Mesoderm | Ets1/2, Frizz, Vasa | 1143 | 10.9 |
| Cluster 4 ● | Ectoderm: Lateral | SoxB1, Wnt8 | 1118 | 10.7 |
| Cluster 5 ● | Undetermined | Fic9, Fbn3 | 924 | 8.8 |
| Cluster 6 ● | Ectoderm: Ventral | GataE, Wnt16, Blimp1, Vasa, FoxA, | 720 | 6.9 |
| Cluster 7 ● | Ectoderm: Oral | Nodal, Lefty, Bmp2/4, Nkx2.1 | 672 | 6.4 |
| Cluster 8 ● | Endoderm: Midgut/hindgut | Cdxl, Blimp1, Wnt3, Wnt8, Brachyury, FoxY3 (annotated as Foxq1) | 595 | 5.7 |
| Cluster 9 ● | Gcm enriched | Gcm | 193 | 1.8 |
| Cluster 10 ● | MifL1 enriched | MifL1, Fos, ribosomal proteins | 46 | 0.4 |

**Table S2. Number of Nanos, Vasa, and FoxY3 expressing cells in cluster 8 (hindgut) and cluster 3 (archenteron) regions.**

| | Nanos | Vasa | FoxY3 | Nanos,Vasa | Vasa,FoxY3 | Nanos,Vasa,FoxY3 | Total |
|---|---|---|---|---|---|---|---|
| **Cluster 8** | 22 | 395 | 221 | 21 | 167 | 9 | 595 |
| **Cluster 3** | 117 | 1099 | 177 | 112 | 167 | 19 | 1143 |

**Table S3. Blastula Cluster Markers**

Click here to download Table S3

**Table S4. MidGastrula Cluster Markers**

Click here to download Table S4

**Table S5. MG Cluster 8 Vasa Positive**

Click here to download Table S5

**Table S6. Harmony Cluster Integration Markers**

Click here to download Table S6

**Supplementary Data 1. PmAnalysis.**

Click here to download Supplementary Data 1